



# Physiological responses of *Skeletonema costatum* to the interactions of seawater acidification and combination of photoperiod and temperature

Hangxiao Li<sup>1,2</sup>, Tianpeng Xu<sup>1,2</sup>, Jing Ma<sup>1,2</sup>, Futian Li<sup>1,2,3\*</sup> & Juntian Xu<sup>1,2,4\*</sup>

<sup>1</sup>Jiangsu Key Laboratory of Marine Biotechnology, Jiangsu Ocean University, Lianyungang 222005, China

<sup>2</sup>Jiangsu Key Laboratory of Marine Bioresources and Environment, Jiangsu Ocean University, Lianyungang 222005, China

<sup>3</sup>Jiangsu Institute of Marine Resources, Lianyungang 222005, China

<sup>4</sup>Co-Innovation Center of Jiangsu Marine Bio-industry Technology, Jiangsu Ocean University, Lianyungang 222005, China

\*Correspondence to: Futian Li (futianli@jou.edu.cn) and Juntian Xu (jtxu@jou.edu.cn)

**Abstract.** Ocean acidification (OA), which is a major environmental change caused by increasing atmospheric CO<sub>2</sub>, has considerable influences on marine phytoplankton. But few studies have investigated interactions of OA and seasonal changes in temperature and photoperiod on marine diatoms. In the present study, a marine diatom *Skeletonema costatum* was cultured under two different CO<sub>2</sub> levels (LC, 400 µatm; HC, 1000 µatm) and three different combinations of temperature and photoperiod length (8:16 L:D with 5 °C, 12:12 L:D with 15 °C, 16:8 L:D with 25 °C), simulating different seasons in typical temperate oceans, to investigate the combined effects of these factors. The results showed that specific growth rate of *S. costatum* increased with increasing temperature and daylength. However, OA showed contrasting effects on growth and photosynthesis under different combinations of temperature and daylength: while positive effects of OA were observed under spring and autumn conditions, it significantly decreased growth (11 %) and photosynthesis (21 %) in winter. In addition, low temperature and short daylength decreased the proteins of PSII (D1, CP47 and RbcL) at ambient pCO<sub>2</sub> level, while OA alleviated the negative effect. These data indicated that future ocean acidification may show differential effects on diatoms in different cluster of other factors.

**Key words.** diatom, growth, photosynthesis, CO<sub>2</sub>, temperature and photoperiod

## 1 Introduction

Ocean acidification (OA) is one of major environmental changes caused by increasing atmospheric CO<sub>2</sub>, which has directly raised from 280 ppm in preindustrial era to higher than 400 ppm at present (Friedlingstein et al., 2019). It is predicted that surface seawater pH would drop 0.3–0.5 and 0.5–0.7 units by the year 2100 and 2300 respectively (Caldeira and Wickett, 2003). It has been suggested that calcifying organisms, such as coral reefs and coccolithophores, are vulnerable to OA due to



the decreased calcification at elevated CO<sub>2</sub> (Albright et al., 2016). The responses of non-calcifying organisms such as diatoms to OA vary widely among taxonomic groups which may be detrimental, negligible or even beneficial (Gao and Campbell, 2014). Consequently, the abundance of marine phytoplankton and community structure might be altered by OA (Gattuso et al., 2015).

Diatoms are ubiquitous photosynthetic phytoplankton which account for about 20 % of global primary productivity, and thus play a crucial role in the global cycling of carbon and silicon (Falkowski et al., 2004). To overcome the limited aqueous CO<sub>2</sub> concentration in seawater, they have developed CO<sub>2</sub>-concentrating mechanisms (CCMs) (Spalding, 2007). Decreased photosynthetic affinity for dissolved inorganic carbon (DIC) and activity of CCM related enzymes are generally found under increased CO<sub>2</sub> condition (Raven and Beardall, 2014). For phytoplankton assemblages, elevated CO<sub>2</sub> could lead to increases in chlorophyll *a* concentrations and the abundance of diatoms (Johnson et al., 2013). Species and strain specificity are observed in studies on physiological responses of diatoms to OA, which might be caused by the balance between positive effects of elevated CO<sub>2</sub> and negative effects of decreased pH (Langer et al., 2009; Li et al., 2016). In addition, acclimation and adaptation processes, i.e. the timescale of diatoms exposed to OA, could also influence the physiological effects of OA (Wu et al., 2014; Li et al., 2017). Moreover, other environmental factors, such as temperature (Seebah et al., 2014), light (Gao et al., 2012), nutrients (Li et al., 2015) and clusters of multiple factors (Xu et al., 2014a; Xu et al., 2014b), are shown to have interaction with OA on diatoms.

Diatoms are widespread across oceans, thus they would experience different photoperiods. Photoperiod controls the total light dose received by phytoplankton and thus could remarkably influence the physiological performance such as growth and lipid content of microalgae (Wahidin et al., 2013). For Antarctic sea ice microalgae *Chlamydomonas* sp., continuous illumination stimulates higher growth and nutrient absorption rates than successive darkness condition (Xu et al., 2014c). Growth rate of *Chlamydomonas reinhardtii* is gradually enhanced following the increasing photoperiod (Hsieh et al., 2018). In contrast, *Alexandrium minutum* grows faster under short daylength relative to longer and even continuous daylength (Wang et al., 2019). Moreover, different photoperiods could influence intracellular carbon demand of microalgae, which has a stronger regulation effect on CCMs compared with effects of changes in CO<sub>2</sub> supply (Rost et al., 2006).

Under the combined influence of photoperiod and OA, physiological performance of phytoplankton might be different from that under single factor. For example, continuous light moderates the negative effect of OA on coccolithophore growth, although species isolated from different regions show diverse responses (Bretherton et al., 2019). The changes of photoperiod are often accompanied by increase or decrease temperature, and impacts of OA on diatoms can also be changed by temperature. For example, under OA condition, decreased metabolic activity is observed in *Phaeodactylum tricorutum* when temperature elevates (Bautista et al., 2018), while elevated temperature enhances the growth rate of *Nitzschia lecointei* (Torstensson et al., 2013).

But limited studies have investigated interactions between OA and combination of temperature and photoperiod (i.e. conditions in different seasons) on diatoms. *Skeletonema costatum* is a widespread, eurythermal and euryhaline diatom species, which frequently causes red tide. We hypothesized the effect of OA on *S. costatum* may be modulated by



65 photoperiod and temperature. In the present study, we investigate the physiological performance of marine diatom  
*Skeletonema costatum* under two different CO<sub>2</sub> levels and three combinations of temperature and photoperiod, which  
simulated different seasons in typical temperate oceans (winter, 5 °C with 8:16 L:D; spring or autumn, 15 °C with 12:12 L:D;  
summer, 25 °C with 16:8 L:D).

## 2 Materials and methods

### 2.1 Culture conditions

70 The diatom *Skeletonema costatum* in this study was isolated from Gaogong Island, Lianyungang, Jiangsu province (34°70'  
74.95"N, 119°49'26.47"E). Before being used in experiments, the cells were cultured in autoclaved natural seawater enriched  
with f / 2 medium (Guillard and Ryther, 1962). Semi-continuous cultures were maintained in 500 ml Erlenmeyer flasks with  
a filter unit (Millex GP, Merck, USA) in order to aerate sterile air. Triplicate independent cultures were set for each treatment  
at the light intensity of 150 μmol photons m<sup>-2</sup> s<sup>-1</sup>.

### 2.2 Experimental setup

75 In order to evaluate effects of pCO<sub>2</sub> levels and different combination of temperature and photoperiod on *S. costatum*, cells  
were cultured under winter condition (5 °C with light: dark cycle of 8:16 h), spring / autumn (15 °C with 12:12 h), summer  
(25 °C with 16:8 h) independently with two pCO<sub>2</sub> levels (400 ppm, LC; 1000 ppm, HC), simulating temperature and  
daylength conditions of different seasons in typical temperate oceans. Temperatures and light intensity (150 μmol photons  
m<sup>-2</sup> s<sup>-1</sup>) were controlled by illumination incubators (GXZ-500B, Ningbo, China). Cells were inoculated in cultures with fresh  
80 medium which was aerated with ambient air (400 ppm) or CO<sub>2</sub>-enriched air (1000 ppm). The high pCO<sub>2</sub> levels were  
manipulated by a CO<sub>2</sub> plant incubator (HP 1000 G-D, Ruihua Instruments, Wuhan, China). Cultures were diluted every 3 d,  
and cells concentrations were controlled below 2×10<sup>5</sup> cell ml<sup>-1</sup> in order to minimize the effect of cell metabolism on  
carbonate chemistry in medium. The changes in culture pH was less than 0.05 during the 3 d. After acclimating to different  
treatments for at least 40 generations, following parameters were measured.

### 85 2.3 Growth measurement

To estimate the growth of *S. costatum*, triplicate samples were collected every 2 d from each treatment and fixed with 10 μl  
Lugol's solution, then a plankton counting chamber (DSJ-01, Xundeng Instruments, Xiamen, China) was used to count cells  
directly under an optical microscope (DM500, Leica, Germany). The specific growth rate was calculated as:  
 $\mu = (\ln N_t - \ln N_0) / (t - t_0)$ , where  $N_t$  represents the cell concentration at time  $t$ ;  $N_0$  represents the cell concentration at time  $t_0$ .



## 90 2.4 Chlorophyll fluorescence measurement

Cells were concentrated by gentle vacuum filtration (< 0.02 MPa) for measurement of rapid light curves (RLCs) under 8 different PAR levels (0, 10, 20, 50, 100, 200, 500, 1000  $\mu\text{mol photons m}^{-2} \text{s}^{-1}$ ) lasting for 10 s each using a hand-held fluorometer (AquaPen-C AP-P 100, Chech). Relative electron transport rates (rETR) of *S. costatum* were measured, and was estimated as Wu, et al. (2010):  $\text{rETR} = \text{PAR} \times Y(\text{II}) \times 0.5$ , where PAR represents the photon flux density of actinic light; 95 Y(II) represents the effective quantum yield of PSII, 0.5 is based on the assumption that PSII receives half of all absorbed quanta. RLCs were fitted as:  $P = \text{PAR} / (a \times \text{PAR}^2 + b \times \text{PAR} + c)$ , where P represents rETR; PAR represents actinic light ( $\mu\text{mol photons m}^{-2} \text{s}^{-1}$ ); a, b and c are model parameters. The relative photoinhibition ratio of rETR was calculated as:  $\text{Inh} (\%) = (\text{rETR}_{\text{max}} - \text{rETR}_x) / \text{rETR}_{\text{max}} \times 100 (\%)$ , where  $\text{rETR}_x$  is the value of rETR at 1000  $\mu\text{mol photons m}^{-2} \text{s}^{-1}$ .

## 2.5 Photosynthesis and respiration measurements

100 Photosynthesis versus light intensity (P-I) curve and photosynthesis versus dissolved inorganic carbon concentration ( $C_i$ ) (P-C) curve of *S. costatum* were measured through a Clark-type oxygen electrode (Oxygraph+, Hansatech, UK), in which temperature was controlled by a thermostatic water bath (DHX-2005, China). For P-C curve, photosynthetic oxygen evolution was measured under same light intensity as culture, provided by a halogen lamp (QVF135, Philips, Netherlands); samples of 50 ml were filtered (< 0.02 MPa) onto a cellulose acetate membrane (Xinya Instruments, Shanghai, China), then 105 were resuspended in 5 ml fresh  $C_i$ -free f / 2 tris buffered medium (pH 8.12), which was then used to determine oxygen evolution rate and cell concentration; the remaining intracellular  $C_i$  was depleted by exposing cells to culture light intensity for 20-30 min. Net photosynthetic rate was determined after adding calculated amounts of  $\text{NaHCO}_3$  stock solution (0.025 M and 0.2 M). The final concentrations of DIC were 0, 0.025, 0.05, 0.1, 0.2, 0.4, 1, 2 and 4 mM. Net photosynthetic rates under different DIC concentration were fitted by Michaelis-Menten equation.

110 As for P-I curve, oxygen consumption rates in darkness and net photosynthetic oxygen evolution under 7 different light intensities (0, 10, 20, 50, 100, 200, 500, 1000  $\mu\text{mol photons m}^{-2} \text{s}^{-1}$ ) were identified. Light intensity was achieved by adjusting the distance between the halogen lamp and oxygen electrode chamber. Photosynthetic rate and light intensity data were fitted according to Henley (1993):  $P = P_m \times \tanh(\alpha \times \text{PAR} / P_m) + R_d$ , where PAR is irradiance, P is photosynthetic rate,  $P_m$  is light-saturated photosynthetic rate,  $\alpha$  is initial slope of P-I curve,  $R_d$  is dark respiration rate.  $I_k$  (saturating irradiance for photosynthesis) and  $I_c$  (light compensation point) were also calculated by:  $I_k = P_m / \alpha$ ,  $I_c = R_d / \alpha$ . 115

## 2.6 Chlorophyll *a* and BSi measurement

Samples were filtered onto GF / F filters (25 mm, Whatman, UK), and chlorophyll *a* were extracted with 4 ml of methanol at 4 °C for 24 h in darkness. An ultraviolet spectrophotometer (Ultrospect 3300 pro, Amersham Bioscience, Sweden) was used to detect the absorption values of supernatant under 632 nm, 665 nm and 750 nm after centrifuging (Biofuge primo R,



120 Thermo, Germany). The chlorophyll *a* concentration of *S. costatum* was calculated by the equation of Ritchie (2006).  
Samples (200 ml) for biogenic silica (BSi) measurement were filtered onto polycarbonate filters (0.8  $\mu\text{m}$ , Merck Millipore,  
Germany) by polysulfone filter funnel (25 mm, Pall Corporation, UK), and filters were then dried at 80°C for 24 h. BSi on  
the filter was digested by 4 ml of 0.2 M NaOH in boiling bath for 40 min, and were neutralized with 1 ml of 1M HCl when  
125 cooled. The supernatant (1 ml) was diluted with 4 ml of milli-Q water, and then 2 ml of molybdate soln and 3 ml of reducing  
agent were added into tubes. The absorption was measured at 810 nm by an ultraviolet spectrophotometer (Ultrospect 3300  
pro, Amersham Bioscience, Sweden) after the color developing for 2-3 h (Brzezinski and Nelson, 1995).

### 2.7 Proteins of PSII measurements

Cells were filtered and resuspended in 2 ml of extracting medium (50 mM Tris-HCl, pH 7.6, 5.0 mM MgCl<sub>2</sub>, 10 mM NaCl,  
0.4 M sucrose, and 0.1 % BSA) according to Ma et al. (2019). After cell disruption and centrifugation, supernatant liquid  
130 was used to measured chlorophyll concentration according to Arnon (1949):  $C = D_{652} \times 1000 \div 34.5 \times T$ , where C represents  
total chlorophyll concentration, D<sub>652</sub> represents absorption value in 652 nm, T represents dilution ratio, 1000 and 34.5 are  
constants. Same concentration of chlorophyll (2.4 micrograms) per lane was used for 12 % sodium dodecyl  
sulfate-polyacrylamide gel electrophoresis (SDS-PAGE, Mini PROTEAN, Bio-rad, America) at 150 V for 1 h, and the  
proteins were transferred into polyvinylidene difluoride (PVDF) membranes which were then immersed in blocking solution  
with antibodies (D1, D2, CP47, Rubisco L; Agrisera) for 1 h, and successively, goat anti-rabbit secondary antibodies were  
135 used. Blots were developed by using enhance chemluminescence luminescence (ECL) reagent and were quantified with a  
chemiluminescence detection system (Tanon 5500, Shanghai, China).

### 2.8 Data analyses

Data were analyzed with IBM SPSS Statistics 24 and are presented as mean  $\pm$  SD (standard deviation). One-way ANOVA  
140 was used to compare differences among combination of temperature and photoperiod treatments. The independent-samples  
*t*-test was applied to compare differences between two pCO<sub>2</sub> levels. General linear model was conducted to assess the  
interactive effects of CO<sub>2</sub> level and combination of temperature and photoperiod on growth rate, rETR, photosynthesis and  
respiration, contents of chlorophyll *a* and BSi and proteins. When *P* values were under 0.05, tukey test was used for *post hoc*  
analysis.

## 145 3 Results

### 3.1 Specific growth rate



150 Growth rate of *S. costatum* ranged from  $0.47 \pm 0.01$  to  $3.22 \pm 0.08$  d<sup>-1</sup> under different treatments and increased significantly with increasing temperature and daylength ( $P < 0.05$ ) regardless the pCO<sub>2</sub> level (Fig. 1). In summer season, elevated pCO<sub>2</sub> showed no significant effects, however, it remarkably influenced the growth rate in other seasons. Elevated pCO<sub>2</sub> enhanced the growth rate by 11 % in spring and autumn ( $P < 0.001$ ), while the reverse pattern was found in winter ( $P < 0.001$ ). General linear model indicated that the season and CO<sub>2</sub> level had a notable interaction on specific growth rate ( $P < 0.001$ , Table 1).

### 3.2 Chlorophyll *a* and BSi contents

155 Under ambient CO<sub>2</sub> condition, chlorophyll *a* content was enhanced by increased temperature and daylength, and the content was 22 % higher in summer compared with winter ( $P = 0.008$ ). When CO<sub>2</sub> was elevated, chlorophyll *a* content in winter was 42 % and 32 % lower than that in spring and summer respectively ( $P = 0.001$ ,  $P = 0.004$ ). Elevated pCO<sub>2</sub> decreased chlorophyll *a* content in winter ( $P = 0.022$ ) while enhanced it in spring ( $P = 0.002$ ) and had no significant impact in summer. A significant interaction between season and CO<sub>2</sub> can be found ( $P < 0.001$ ) (Table 1).

160 A different trend was detected for BSi content (Table 2). Under ambient pCO<sub>2</sub>, BSi content decreased with higher temperature along with longer daylength and the value in winter was significantly higher than that in spring and summer ( $P=0.005$ ,  $0.002$  respectively). Higher pCO<sub>2</sub> decreased BSi significantly in winter ( $P = 0.016$ ) and spring ( $P = 0.007$ ) while had no significant influence on the content in summer ( $P = 0.3$ ). There is a significant interaction between season and CO<sub>2</sub> on BSi content ( $P < 0.05$ ) (Table 1).

### 3.3 Photosynthesis and respiration

165 Combination of temperature and photoperiod in different seasons had a significant effect on  $V_{\max}$  ( $P < 0.001$ , Table 1), cells under spring season condition had the highest  $V_{\max}$  at both pCO<sub>2</sub> levels, but the lowest  $V_{\max}$  was found in winter at elevated pCO<sub>2</sub> and in summer at ambient pCO<sub>2</sub>. Elevated pCO<sub>2</sub> significantly enhanced the values in higher temperature and longer daylength treatments (129 % for spring, 130 % for summer when compared with ambient CO<sub>2</sub> level). With respect to  $K_m$ , different season had no significant effect on it at ambient pCO<sub>2</sub>, while  $K_m$  in summer was lowest among the seasons at elevated pCO<sub>2</sub> (70 % and 69 % lower than winter and spring respectively). Elevated pCO<sub>2</sub> had significant influences on  $K_m$  under same season besides summer and the values increased by 143 % and 113 % in winter and spring respectively when compared with low pCO<sub>2</sub> ( $P = 0.021$ ,  $P = 0.003$  in winter and spring). Interaction between CO<sub>2</sub> and combination of temperature and photoperiod on parameters of P-C curves were detected (Table 1).

175 Higher temperature and prolonged daylength had a main effect on  $P_{\max}$ ,  $R_d$ ,  $I_k$  and  $I_c$ . However, elevated pCO<sub>2</sub> instead of season had main effect on  $\alpha$  (Table 1).  $P_{\max}$  was enhanced when temperature increasing with prolonged daylength ( $P < 0.05$ ) except when the summer season was compared with spring condition at elevated pCO<sub>2</sub>. Effects of elevated pCO<sub>2</sub> was only



observed in spring ( $P = 0.03$ ).  $I_k$  increased remarkably in summer under both  $p\text{CO}_2$  treatments which was similar as  $R_d$  at elevated  $p\text{CO}_2$  ( $P < 0.05$ ). There was a significant interaction between  $\text{CO}_2$  and combination of temperature and photoperiod on  $R_d$  (Table 1).

### 180 3.4 Chlorophyll fluorescence

At higher  $p\text{CO}_2$  level,  $r\text{ETR}_{\text{max}}$  values were significantly different among different seasons ( $P < 0.05$ ), and the value in spring was highest (52 % and 14% higher than winter and summer, Table 3). Elevated  $p\text{CO}_2$  decreased  $r\text{ETR}_{\text{max}}$  in winter and summer ( $P < 0.001$  in winter,  $P = 0.01$  in summer). Interactions between the two factors were detected on  $r\text{ETR}_{\text{max}}$  ( $P < 0.001$ , Table 1). Photoinhibitions were found in RLCs of cells under all treatments. As the season processed from winter to summer, photoinhibitions were alleviated significantly in both  $p\text{CO}_2$  levels ( $P < 0.05$ ). In spring, the inhibition at higher  $p\text{CO}_2$  was significantly decreased compared with ambient  $p\text{CO}_2$  condition ( $P = 0.039$ , Table 3).

### 3.5 PSII protein concentrations

The concentrations of key PSII proteins (PsbA (D1), PsbD (D2), PsbB (CP47), and RbcL) were quantified in different seasons under ambient and elevated  $\text{CO}_2$  conditions. D1 and D2 proteins are located in reaction center, while CP47 is a junction of antenna, and RbcL is related to the function of  $Q_A$ . Values of Actin were divided by other densitometric scanning values of protein to calculate Gray-scale values. At ambient  $p\text{CO}_2$ , the highest contents of all four proteins were detected in spring. Except D2 protein, elevated  $p\text{CO}_2$  significantly enhanced the PSII protein contents in winter ( $P = 0.010, 0.014, 0.016$  for D1, RbcL, and CP47 respectively). In addition, higher  $p\text{CO}_2$  led to reduction of D2 but increase of D1 in Spring ( $P = 0.003, 0.047$  respectively). When  $p\text{CO}_2$  elevated, the content of CP47 were increased significantly in summer ( $P = 0.034$ ).

## 195 4. Discussion

Phytoplankton like diatoms have already evolved several strategies to cope with different temperature and daylength in temperate oceans, where variations of season are evident. However, the ongoing elevated  $p\text{CO}_2$  combining with changes in temperature and daylength is a new stress on diatoms and we know little about their interactions. Therefore, we examined the combined effects of  $p\text{CO}_2$  and seasonal changes in temperature and photoperiod on the physiological performance of a typical marine diatom *S. costatum*.

### 4.1 Physiological responses of *S. costatum* to different combinations of temperature and photoperiod

In the present study, the growth rate of *S. costatum* increased with increasing temperature and daylength regardless of the  $p\text{CO}_2$  level (Fig. 1). Precious studies showed that most phytoplankton, such as *Chlamydomonas reinhardtii*, *Trichodesmium*



205 or *Alexandrium catenella*, grew faster under prolonged photoperiods (Cai and Gao, 2015) although *Alexandrium minutum* grew faster under shorter photoperiods (Wang et al., 2019). For *S. costatum*, a remarkably higher contribution of  $\text{HCO}_3^-$  to the overall carbon uptake was observed under light dark cycles compared with continuous light, and a shorter photoperiod led to lower photosynthetic affinity for inorganic carbon (Rost et al., 2006). Basically, the Chl *a* quota in microalgae increases with decreasing daylength, however, our results exhibited inverse pattern (Table 2). The inconsistency might be caused by the different temperatures set in studies, which is another main environmental factor affecting the growth of  
210 diatoms.

Increasing temperature may lead to various changes in growth rate depending on whether the temperature is optimal for the species. For *S. costatum*, its growth rate has been shown to increase with temperature up to 30 °C (Ebrahimi and Salarzadeh, 2016). Zhang et al. (2020) also found that the growth rate of *S. costatum* could increase with temperature from 5 °C to 30 °C and then drop sharply. The underlying mechanism is that elevated temperature promotes *S. costatum* metabolic rates when  
215 nutrients are abundant. This could be shown by the relationship between respiration and growth. Higher mitochondrial respiration can result in higher growth rate theoretically (Geider and Osborne, 1989), since this process provides ATP and carbon skeletons (Raven et al., 2017). It seems that temperature shows the dominant effect compared with daylength.

Lavaud et al. (2016) indicated that PSII activity and phosphorylation of thylakoid protein may play a crucial role in controlling the change of the photosynthetic activity. Rubisco is an important enzyme for C fixation, psychrophilic diatoms  
220 utilize increasing abundance of RbcL protein to maintain high cellular enzymatic rates and growth rate at low temperature (Young et al., 2015). However, for diatoms in temperate area, the amount of RbcL protein decreased in low temperature along with short daylength compared with higher temperature and longer daylength in our results. Low abundance of RbcL was in line with slower growth rate in winter condition.

#### 4.2 Effect of ocean acidification under different seasons

225 Our results showed that the impacts of elevated  $\text{pCO}_2$  on *S. costatum* depended on seasonal changes in temperature and photoperiod. High  $\text{pCO}_2$  had but enhanced the growth of *S. costatum* in spring and reduced it in winter, while no significant effects were detected in summer (Fig. 1).  $\text{CO}_2$  concentration mechanisms (CCMs) is energy-dependent and high  $\text{pCO}_2$  down-regulate CCMs of most phytoplankton including *S. costatum*, so the saved energy could be used for growth (Raven et al., 2017). Higher initial slope of the P-I curve at elevated  $\text{pCO}_2$  might be partly responsible for the higher growth rate  
230 compared with that at ambient  $\text{pCO}_2$  (Table 3). But in winter, growth decreased under OA condition, although photosynthesis and respiration had no significant changes. This is because the combination of biochemical and biophysical CCMs may cause the lack of a positive response to elevated  $\text{pCO}_2$  under near-optimal growth conditions (Passow, 2015). In addition, when other environmental factors are stressful, the sensitivity of diatoms to  $\text{CO}_2$  and temperature is prominent (Taucher et al., 2015). The shorter daylength and low temperature simulating winter condition in present study can be seen as stressors,  
235 under which *S. costatum* was more sensitive to elevated  $\text{pCO}_2$ . When temperature and photoperiod are optimal, positive or





neutral effects of higher pCO<sub>2</sub> were observed. However, different patterns were reported for other species, such as *E. huxleyi* and the macroalgae *Ulva linza* (Bretherton et al., 2019; Yue et al., 2019). For these two species, reduced growth rate at elevated pCO<sub>2</sub> were found when the daylength was longest. High temperature might accelerate nutrient uptake and metabolic rates, which may alleviate the negative effects of longer daylength under higher pCO<sub>2</sub> environment (Bretherton et al., 2019; Yue et al., 2019). Maximum photosynthetic rate increased significantly under higher pCO<sub>2</sub> in spring condition. This was consistent with the higher photosynthetic efficiency and growth rate (Table 3, Fig. 1). Meanwhile, K<sub>m</sub> increased under high CO<sub>2</sub> concentration which means the affinity for CO<sub>2</sub> decrease and thus CCMs are down-regulated.

Silicification directly relates to cell division and growth, and is independent of photoperiod (Brzezinski, 1992). BSi contents generally increased with decreasing growth rate when any limiting factors such as temperature, light or ammonium exist (Martin et al., 2000). In the present study, elevated pCO<sub>2</sub> mitigated the negative effects of temperature and photoperiod limitation on BSi content (Table 2). Higher BSi contents in winter under ambient CO<sub>2</sub> condition can intensify the ballasting effects and thus impact the sinking rate of organic matters produced by diatoms.

Higher pCO<sub>2</sub> induced higher photosynthetic efficiency in PSII, with increased contents of proteins in winter. Proteins will be degraded and synthesized rapidly after damage. Therefore, the decline in growth under winter condition might result from the increased metabolic costs of photoprotection and elevated D1 turnover under the combination of short daylength limitation and low temperature (Hoppe et al., 2015).

For diatoms, a mounting body of studies has pay attention to the effect of interactions of ocean acidification and other environmental factors such as light intensity, UV, temperature, nutrient limitation, salinity or photoperiod (Gao et al., 2012; Yue et al., 2019), and the results showed positive, negative or neutral effects (Xu et al., 2014c; Li et al., 2017). However, few studies combined elevated pCO<sub>2</sub> with seasonal changes in seawater physical and chemical characters on marine diatoms. In this study, temperature and photoperiod were chosen as seasonal factors to investigate the combined effects of pCO<sub>2</sub> and these two factors on physiology of *S. costatum*. Our results suggested temperature and photoperiod could mediate effects of elevated pCO<sub>2</sub> on the typical diatom *S. costatum*. Positive effects of OA on growth and photosynthesis were observed in spring and autumn, while negative effects were found in winter condition. To better understand how global climate changes would affect marine diatoms in the future, it is necessary to explore the interactive effects of ocean acidification with seasonal changes in seawater characters.

### Author Contributions

JX and FL conceived and designed the experiments; HL and TX carried out the experiments; HL, FL and JX analyzed data; HL wrote the draft of the paper; FL, JM and JX revised the manuscript and approved this version for submission.

### Competing interests



The authors declare that they have no conflict of interest.

## Acknowledgements

This study was funded by China Postdoctoral Science Foundation (2019M661766), the Six Talents Peaks in Jiangsu Province (JY-086), Postgraduate Research & Practice Innovation Program of Jiangsu Province (KYCX19\_2290), the Priority Academic Program Development of Jiangsu Higher Education Institutions.

## References

- Albright, R., Caldeira, L., Hosfelt, J., Kwiatkowski, L., Maclaren, K. J., Mason, B., Nebuchina, Y., Ninokawa, A., Pongratz, J., Ricke, K. L., Rivlin, T., Schneider, K., Sesboue, M., Shamberger, K. E. F., Silverman, J., Wolfe, K., Zhu, K., and Caldeira K.: Reversal of ocean acidification enhances net coral reef calcification, *Nature*, 531, 362–365, doi: 10.1038/nature17155, 2016.
- Arnon D. I.: Copper enzymes in isolated chloroplasts. polyphenoloxidase in *Beta vulgaris*, *Plant Physiol.*, 24, 1–15, doi: 10.1104/pp.24.1.1, 1949.
- Bautistachamizo, E., Sendra, M., Cid, A., Seoane, M., Orte, M. R. D., and Riba, I.: Will temperature and salinity changes exacerbate the effects of seawater acidification on the marine microalga *Phaeodactylum tricorutum*? *Sci. Total Environ.*, 634, 87–94, doi: 10.1016/j.scitotenv.2018.03.314, 2018.
- Behrenfeld, M. J., Prasil, O., Kolber, Z., Babin, M., and Falkowski, P.: Compensatory changes in Photosystem II electron turnover rates protect photosynthesis from photoinhibition, *Photosyn. Res.*, 58, 259–268, doi: 10.1023/A:1006138630573, 1998.
- Bretherton, L., Poulton, A. J., Lawson, T., Rukminasari, N., Balestreri, C., Schroeder, D. C., Moore, C. M., and Suggett, D. J.: Day length as a key factor moderating the response of coccolithophore growth to elevated pCO<sub>2</sub>, *Limnol. Oceanogr.*, 64, 1284–1296, doi: 10.1002/lno.11115, 2019.
- Brzezinski, M. A., and Nelson, D. M.: The annual silica cycle in the Sargasso Sea near Bermuda, *Deep Sea Research Part I: Oceanographic Research Papers*, 42, 1215–1237, doi: 10.1016/0967-0637(95)93592-3, 1995.
- Cai, X., and Gao, K.: Levels of daily light doses under changed day-night cycles regulate temporal segregation of photosynthesis and N<sub>2</sub> fixation in the Cyanobacterium *Trichodesmium erythraeum* IMS101, *PLoS One*, 10, e0135401, doi: 10.1371/journal.pone.0135401, 2015.
- Caldeira, K., and Wickett, M. E.: Oceanography: anthropogenic carbon and ocean pH, *Nature*, 425, 365–365, doi: 10.1038/425365a, 2003.
- Chen, X., and Gao, K.: Characterization of diurnal photosynthetic rhythms in the marine diatom *Skeletonema costatum* grown in synchronous culture under ambient and elevated CO<sub>2</sub>, *Funct. Plant Biol.*, 31, 399–404, doi: 10.1071/FP03240,



- 2004.
- Ebrahimi, E., and Salarzadeh, A.: The effect of temperature and salinity on the growth of *Skeletonema costatum* and *Chlorella capsulata* in vitro, *International Journal of Life Sciences*, 10, 40–44, doi: 10.3126/ijls.v10i1.14508, 2016.
- Eilers, P. H. C. and Petters, J. C. H.: A model for the relationship between light intensity and the rate of photosynthesis in phytoplankton, *Ecol. Modell.*, 42, 199–215, doi: 10.1016/0304-3800(88)90057-9, 1988.
- 300 Falkowski, P. G., Katz, M. E., Knoll, A. H., Quigg, A., Raven, J. A., Schofield, O., and Taylor, F. J. R.: The evolution of modern eukaryotic phytoplankton, *Science*, 305, 354–360, doi: 10.1126/science.1095964, 2004.
- Friedlingstein P, Jones M W, Osullivan M, Andrew, R. M., Hauck, J., Peters, G. P., Peters, W., Pongratz, J., Sitch, S., Quere, C. L., Bakker, D. C. E., Canadell, J. G., Ciais, P., Jackson, R. B., Anthoni, P., Barbero, L., Bastos, A., Bastrikov, V.,
- 305 Becker, M., Bopp, L., Buitenhuis, E. T., Chandra, N., Chevallier, F., Chini, L. P., Currie, K. I., Feely, R. A., Gehlen, M., Gilfillan, D., Gkritzalis, T., Goll, D., Gruber, N., Gutekunst, S., Harris, I., Haverd, V., Houghton, R. A., Hurtt, G. C., Ilyina, T., Jain, A. K., Joetzer, E., Kaplan, J. O., Kato, E., Goldewijk, K. K., Korsbakken, J. I., Landschutzer, P., Lauvset, S. K., Lefevre, N., Lenton, A., Lienert, S., Lombardozzi, D., Marland, G., Mcguire, P. C., Melton, J. R., Metzl, N., Munro, D. R., Nabel, J. E. M. S., Nakaoka, S. I., Neill, C., Omar, A. M., Ono, T., Peregon, A., Pierrot, D., Poulter, B., Rehder, G.,
- 310 Resplandy, L., Robertson, E., Rodenbeck, C., Seferian, R., Schwinger, J., Smith, N., Tans, P. P., Tian, H., Tilbrook, B., Tubiello, F. N., Werf, G. R. V. D., Wiltshire, A., Zaehle, S.: Global carbon budget 2019, *Earth Syst. Sci. Data*, 11, 1783–1838, doi: 10.5194/essd-11-1783-2019, 2019.
- Gao, G., Xia, J., Yu, J., Fan, J., and Zeng, X.: Regulation of inorganic carbon acquisition in a red tide alga (*Skeletonema costatum*): the importance of phosphorus availability, *Biogeosciences*, 15, 4871–4882, doi: 10.5194/bg-15-4871-2018,
- 315 2018.
- Gao, K., and Campbell, D. A.: Photophysiological responses of marine diatoms to elevated CO<sub>2</sub> and decreased pH: a review, *Funct. Plant Biol.*, 41, 449–459, doi: 10.1071/FP13247, 2014.
- Gao, K., Xu, J., Gao, G., Li, Y., Hutchins, D. A., Huang, B., Wang, L., Zheng, Y., Jin, P., Cai, X., Hader, D., Li, W., Xu, K., Liu, N., and Riebesell, U.: Rising CO<sub>2</sub> and increased light exposure synergistically reduce marine primary productivity, *Nat. Clim. Chang.*, 2, 519–523, doi: 10.1038/NCLIMATE1507, 2012.
- 320 Gattuso, J. P., Magnan, A., Bille, R., Cheung, W., Howes, E. L., Joos, F., Allemand, D., Bopp, L., Cooley, S. R., Eakin, C. M., Hoeghuldberg, O., Kelly, R. P., Portner, H., Rogers, A. D., Baxter, J. M., Laffoley, D., Osborn, D., Rankovic, A., Rochette, J., Sumaila, U. R., Treyer, S., and Turley, C. M.: Contrasting futures for ocean and society from different anthropogenic CO<sub>2</sub> emissions scenarios, *Science*, 349, aac4722, doi: 10.1126/science.aac4722, 2015.
- 325 Geider, R. J., and Osborne, B. A.: Respiration and microalgal growth: a review of the quantitative relationship between dark respiration and growth, *New Phytol.*, 112, 327–341, doi: 10.1111/j.1469-8137.1989.tb00321.x, 1989.
- Guillard, R. R. L., and Ryther, J. H.: Studies of marine planktonic diatoms: I. *Cyclotella nana* Hustedt, and *Detonula confervacea* (Cleve) Gran, *Can. J. Microbiol.*, 8, 229–239, doi: 10.1139/m62-029, 1962.
- Hartmann, J., West, A. J., Renforth, P., Kohler, P., Rocha, C. L. D. L., Wolfgladrow, D., Durr, H. H., and Scheffran, J.:



- 330 Enhanced chemical weathering as a geoengineering strategy to reduce atmospheric carbon dioxide, supply nutrients, and mitigate ocean acidification, *Rev. Geophys.*, 51, 113–149, doi: 10.1002/rog.20004, 2013.
- Henley, W. J.: Measurement and interpretation of photosynthetic light-response curves in algae in the context of photoinhibition and diel changes, *J. Phycol.*, 29, 729–739, doi: 10.1111/j.0022-3646.1993.00729.x, 1993.
- Hoppe, C. J. M., Holtz, L. M., Trimborn, S., and Rost, B.: Ocean acidification decreases the light-use efficiency in an Antarctic diatom under dynamic but not constant light, *New Phytol.*, 207, 159–171, doi: 10.1111/nph.13334, 2015.
- 335 Johnson, V. R., Brownlee, C., Rickaby, R. E. M., Graziano, M., Milazzo, M., and Hallspencer, J. M.: Responses of marine benthic microalgae to elevated CO<sub>2</sub>, *Mar. Biol.*, 160, 1813–1824, doi: 10.1007/s00227-011-1840-2, 2013.
- Langer, G., Nehrke, G., Probert, I., Ly, J., and Ziveri, P.: Strain-specific responses of *Emiliania huxleyi* to changing seawater carbonate chemistry, *Biogeosciences*, 6, 2637–2646, doi: 10.5194/bg-6-2637-2009, 2009.
- 340 Lavaud, J., Six, C., and Campbell, D. A.: Photosystem II repair in marine diatoms with contrasting photophysiology, *Photosyn. Res.*, 127, 189–199, doi: 10.1007/s11120-015-0172-3, 2016.
- Li, F., Beardall, J., Collins, S., and Gao, K.: Decreased photosynthesis and growth with reduced respiration in the model diatom *Phaeodactylum tricornutum* grown under elevated CO<sub>2</sub> over 1800 generations, *Glob. Chang. Biol.*, 23, 127–137, doi: 10.1111/gcb.13501, 2017.
- 345 Li, F., Beardall, J., and Gao, K.: Diatom performance in a future ocean: interactions between nitrogen limitation, temperature, and CO<sub>2</sub>-induced seawater acidification, *ICES J. Mar. Sci.*, 75, 1451–1464, doi: 10.1093/icesjms/fsx239, 2018.
- Li, F., Wu, Y., Hutchins, D. A., Fu, F., and Gao, K.: Physiological responses of coastal and oceanic diatoms to diurnal fluctuations in seawater carbonate chemistry under two CO<sub>2</sub> concentrations, *Biogeosciences*, 13, 6247–6259, doi: 10.5194/bg-2016-281, 2016.
- 350 Li, W., Gao, K., and Beardall, J.: Interactive effects of ocean acidification and nitrogen-limitation on the diatom *Phaeodactylum tricornutum*, *PLoS One*, 7, e51590, doi: 10.1371/journal.pone.0051590, 2012.
- Li, W., Gao, K., and Beardall J.: Nitrate limitation and ocean acidification interact with UV-B to reduce photosynthetic performance in the diatom *Phaeodactylum tricornutum*, *Biogeosciences*, 12, 2383–2393, doi: 10.5194/bg-12-2383-2015, 2015.
- 355 Ma, J., Wang, W., Liu, X., Wang, Z., Gao, G., Wu, H., Li, X., and Xu, J.: Zinc toxicity alters the photosynthetic response of red alga *Pyropia yezoensis* to ocean acidification, *Environ. Sci. Pollut. Res.*, 27, 3202–3212, doi: 10.1007/s11356-019-06872-7, 2020.
- Malviya, S., Scalco, E., Audic, S., Vincent, F., Veluchamy, A., Poulain, J., Wincker, P., Iudicone, D., Vargas, C. D., Bittner, L., Zingone, A., and Bowler, C.: Insights into global diatom distribution and diversity in the world’s ocean, *Proc. Natl. Acad. Sci.*, 113, E1516–E1525, doi: 10.1073/pnas.1509523113, 2016.
- 360 Martin-Je’ze’quel, V., Hildebrand, M. and Brzezinski, M. A.: Silicon metabolism in diatoms: implications for growth, *J. Phycol.*, 36, 821–840, doi: 10.1046/j.1529-8817.2000.00019.x, 2000.
- Meyers, M. T., Cochlan, W. P., and Carpenter, E. J.: Effect of ocean acidification on the nutritional quality of marine



- phytoplankton for copepod reproduction, *PloS One*, 14, e0217047, doi: 10.1371/journal.pone.0217047, 2019.
- 365 Passow, U., and Laws, E. A.: Ocean acidification as one of multiple stressors: growth response of *Thalassiosira weissflogii* (diatom) under temperature and light stress, *Mar. Ecol. Prog. Ser.*, 541, 75–90, doi: 10.3354/meps11541, 2015.
- Raven, J. A., and Beardall, J.: CO<sub>2</sub> concentrating mechanisms and environmental change, *Aquat. Bot.*, 118, 24–37, doi: 10.1016/j.aquabot.2014.05.008, 2014.
- Raven, J. A., Beardall, J., and Sánchez-Baracaldo, P.: The possible evolution and future of CO<sub>2</sub>-concentrating mechanisms, *J.*  
370 *Exp. Bot.*, 68, 3701–3716, doi: 10.1093/jxb/erx110, 2017.
- Raven, J. A., and Johnston, A. M.: Mechanisms of inorganic-carbon acquisition in marine phytoplankton and their implications for the use of other resources, *Limnol. Oceanogr.*, 36, 1701–1714, doi: 10.4319/lo.1991.36.8.1701, 1991.
- Ritchie, R. J.: Consistent sets of spectrophotometric chlorophyll equations for acetone, methanol and ethanol solvents, *Photosyn.Res.*, 89, 27–41, doi: 10.1007/s11120-006-9065-9, 2006.
- 375 Rost, B., Riebesell, U., and Sültemeyer, D.: Carbon acquisition of marine phytoplankton: effect of photoperiod length, *Limnol. Oceanogr.*, 51, 12–20, doi: 10.4319/lo.2006.51.1.0012, 2006.
- Seebah, S., Fairfield, C., Ullrich, M. S., and Passow, U.: Aggregation and sedimentation of *Thalassiosira weissflogii* (diatom) in a warmer and more acidified future ocean, *PloS One*, 9, e112379, doi: 10.1371/journal.pone.0112379, 2014.
- Spalding, M. H.: Microalgal carbon-dioxide-concentrating mechanisms: *Chlamydomonas* inorganic carbon transporters, *J.*  
380 *Exp. Bot.*, 59, 1463–1473, doi: 10.1093/jxb/erm128, 2007.
- Taucher, J., Jones, J., James, A., Brzezinski, M. A., Carlson, C. A., Riebesell U., and Passow, U.: Combined effects of CO<sub>2</sub> and temperature on carbon uptake and partitioning by the marine diatoms *Thalassiosira weissflogii* and *Dactyliosolen fragilissimus*, *Limnol. Oceanogr.*, 60, 901–919, doi: 10.1002/lno.10063, 2015.
- Torstensson, A., Hedblom, M., Andersson, J., Andersson, M. X., and Wulff, A.: Synergism between elevated pCO<sub>2</sub> and  
385 temperature on the Antarctic sea ice diatom *Nitzschia lecointei*, *Biogeosciences*, 10, 6391–6401, doi: 10.5194/bg-10-6391-2013, 2013.
- Wahidin, S., Idris, A., and Shaleh, S. R. M.: The influence of light intensity and photoperiod on the growth and lipid content of microalgae *Nannochloropsis* sp., *Bioresour. Technol.*, 129, 7–11, doi: 10.1016/j.biortech.2012.11.032, 2013.
- Wang, H., Zhang, B., Song, X., Jian, X. Tang, C. Campbell, D. A. Lin, Q., and Li, G.: High antioxidant capability interacts  
390 with respiration to mediate two *Alexandrium* species growth exploitation of photoperiods and light intensities, *Harmful Algae*, 82, 26–34, doi: 10.1016/j.hal.2018.12.008, 2019.
- Wu, Y., Campbell, D. A., Irwin, A. J., Suggett, D. J., and Finkel, Z. V.: Ocean acidification enhances the growth rate of larger diatoms, *Limnol. Oceanogr.*, 59, 1027–1034, doi: 10.4319/lo.2014.59.3.1027, 2014.
- Xu, K., Fu, F., and Hutchins, D. A.: Comparative responses of two dominant Antarctic phytoplankton taxa to interactions  
395 between ocean acidification, warming, irradiance, and iron availability, *Limnol. Oceanogr.*, 59, 1919–1931, doi: 10.4319/lo.2014.59.6.1919, 2014a.
- Xu, J., Gao, K., Li, Y., and Hutchins, D. A.: Physiological and biochemical responses of diatoms to projected ocean changes,



Mar. Ecol. Prog. Ser., 515, 73–81, doi: 10.3354/meps11026, 2014b.

400 Xu, D., Wang, Y., Fan, X., Wang, D., Ye, N., Zhang, X., Mou, S., Guan, Z., and Zhuang, Z.: Long-term experiment on physiological responses to synergetic effects of ocean acidification and photoperiod in the Antarctic sea ice algae *Chlamydomonas sp.* ICE-L, Environ. Sci. Technol., 48, 7738–7746, doi: 10.1021/es404866z, 2014c.

Young, J. N., Goldman, J. A. L., Kranz, S. A., Tortell, P. D., and Morel, F. M. M.: Slow carboxylation of Rubisco constrains the rate of carbon fixation during Antarctic phytoplankton blooms, New Phytol., 205, 172–181, doi: 10.1111/nph.13021, 2015.

405 Yue, F., Gao, G., Ma, J., Wu, H., Li, X., and Xu, J.: Future CO<sub>2</sub>-induced seawater acidification mediates the physiological performance of a green alga *Ulva linza* in different photoperiods, PeerJ, 7, e7048, doi: 10.7717/peerj.7048, 2019.

Zhang, L., Li, H., Wu, M., Li, F., and Xu, J.: Effects of seawater acidification on photosynthetic physiological characteristics of *Skeletonema costatum* at different temperatures, J. Ocean Univ. China, 29, 1–7, doi: 10.3969/j.issn.2096-8248.2020.01.001, 2020.

410



**Table 1: Significance test results of growth, Chl *a*, BSi, photosynthetic and respiration rates, parameters of P-I, P-C and RLCs curves for combination of temperature and photoperiod (season), CO<sub>2</sub>, and their interactions.**

Parameter	Season		CO <sub>2</sub>		Season * CO <sub>2</sub>	
	F	<i>p</i>	F	<i>p</i>	F	<i>p</i>
Specific growth rate	7662.1	<b>&lt;0.001</b>	0.3	0.569	27.3	<b>&lt;0.001</b>
BSi	22.6	<b>&lt;0.001</b>	22.5	<b>&lt;0.001</b>	10.9	<b>&lt;0.001</b>
P <sub>m</sub>	85.5	<b>&lt;0.001</b>	6.3	<b>0.028</b>	3.4	0.069
$\alpha$	1.8	0.211	6.2	<b>0.028</b>	1.5	0.262
R <sub>d</sub>	7.3	<b>0.010</b>	3.3	0.097	4.2	<b>0.044</b>
V <sub>max</sub>	88.4	<b>&lt;0.001</b>	136.8	<b>&lt;0.001</b>	49.9	<b>&lt;0.001</b>
K <sub>m</sub>	20.5	<b>&lt;0.001</b>	35.7	<b>&lt;0.001</b>	6.7	<b>0.011</b>
rETR <sub>max</sub>	85.3	<b>&lt;0.001</b>	98.5	<b>&lt;0.001</b>	26.0	<b>&lt;0.001</b>

415 **Table 2: Chl *a* and BSi contents of *S. costatum* acclimated to ambient and elevated pCO<sub>2</sub> in different seasons. The data are mean  $\pm$  SD values of triplicate cultures (n = 3). Different lowercases represent significant differences (*P* < 0.05) between two CO<sub>2</sub> levels under same season (*t*-test).**

Treatments	Chl <i>a</i>		BSi	
	LC	HC	LC	HC
Winter	0.18 $\pm$ 0.008 <sup>a</sup>	0.15 $\pm$ 0.013 <sup>b</sup>	0.035 $\pm$ 0.003 <sup>a</sup>	0.025 $\pm$ 0.003 <sup>b</sup>
Spring / Autumn	0.19 $\pm$ 0.007 <sup>a</sup>	0.26 $\pm$ 0.014 <sup>b</sup>	0.025 $\pm$ 0.002 <sup>a</sup>	0.019 $\pm$ 0.001 <sup>b</sup>
Summer	0.22 $\pm$ 0.015 <sup>a</sup>	0.23 $\pm$ 0.024 <sup>a</sup>	0.023 $\pm$ 0.001 <sup>a</sup>	0.024 $\pm$ 0.002 <sup>a</sup>

420 **Table 3: Photosynthetic parameters of P-I and rapid light curves for *S. costatum* acclimated to ambient and elevated pCO<sub>2</sub> in different seasons. P<sub>max</sub> is the maximum net photosynthetic rate,  $\alpha$  is the photosynthetic efficiency, R<sub>d</sub> is the dark respiration rate, I<sub>k</sub> is the photosynthetic saturated light intensity, I<sub>c</sub> is light compensation point, rETR<sub>max</sub> is the maximum relative electron rate and Inh is the relative photoinhibition ratio of rETR. Different lowercases represent significant differences (*P* < 0.05) between two CO<sub>2</sub> levels under same season (*t*-test).**

	P <sub>max</sub>	$\alpha$	R <sub>d</sub>	I <sub>k</sub>	I <sub>c</sub>	rETR <sub>max</sub>	Inh (%)
Winter-LC	0.13 $\pm$ 0.01 <sup>a</sup>	0.0012 $\pm$ 0.00007 <sup>a</sup>	0.011 $\pm$ 0.006 <sup>a</sup>	112.4 $\pm$ 17.3 <sup>a</sup>	9.8 $\pm$ 5.1 <sup>a</sup>	59.0 $\pm$ 1.76 <sup>a</sup>	147.3 $\pm$ 6.7 <sup>a</sup>
Winter-HC	0.11 $\pm$ 0.02 <sup>a</sup>	0.0012 $\pm$ 0.00045 <sup>a</sup>	0.003 $\pm$ 0.002 <sup>a</sup>	97.5 $\pm$ 21.7 <sup>a</sup>	7.2 $\pm$ 3.3 <sup>a</sup>	40.3 $\pm$ 1.43 <sup>b</sup>	135.0 $\pm$ 16.8 <sup>a</sup>
Spring-LC	0.23 $\pm$ 0.04 <sup>a</sup>	0.0011 $\pm$ 0.00012 <sup>a</sup>	0.007 $\pm$ 0.003 <sup>a</sup>	204.1 $\pm$ 28.0 <sup>a</sup>	5.7 $\pm$ 1.9 <sup>a</sup>	67.4 $\pm$ 1.59 <sup>a</sup>	68.7 $\pm$ 6.9 <sup>a</sup>
Spring-HC	0.31 $\pm$ 0.03 <sup>b</sup>	0.0016 $\pm$ 0.00019 <sup>b</sup>	0.019 $\pm$ 0.007 <sup>a</sup>	192.3 $\pm$ 19.9 <sup>a</sup>	11.1 $\pm$ 3.5 <sup>a</sup>	61.6 $\pm$ 3.77 <sup>a</sup>	54.5 $\pm$ 4.3 <sup>b</sup>
Summer-LC	0.35 $\pm$ 0.05 <sup>a</sup>	0.0011 $\pm$ 0.00009 <sup>a</sup>	0.016 $\pm$ 0.008 <sup>a</sup>	336.7 $\pm$ 66.3 <sup>a</sup>	14.5 $\pm$ 7.1 <sup>a</sup>	57.1 $\pm$ 0.04 <sup>a</sup>	28.9 $\pm$ 4.3 <sup>a</sup>
Summer-HC	0.41 $\pm$ 0.05 <sup>a</sup>	0.0013 $\pm$ 0.00018 <sup>a</sup>	0.032 $\pm$ 0.011 <sup>a</sup>	322.8 $\pm$ 36.1 <sup>a</sup>	25.4 $\pm$ 10.5 <sup>a</sup>	53.8 $\pm$ 1.29 <sup>b</sup>	27.1 $\pm$ 2.7 <sup>a</sup>

425

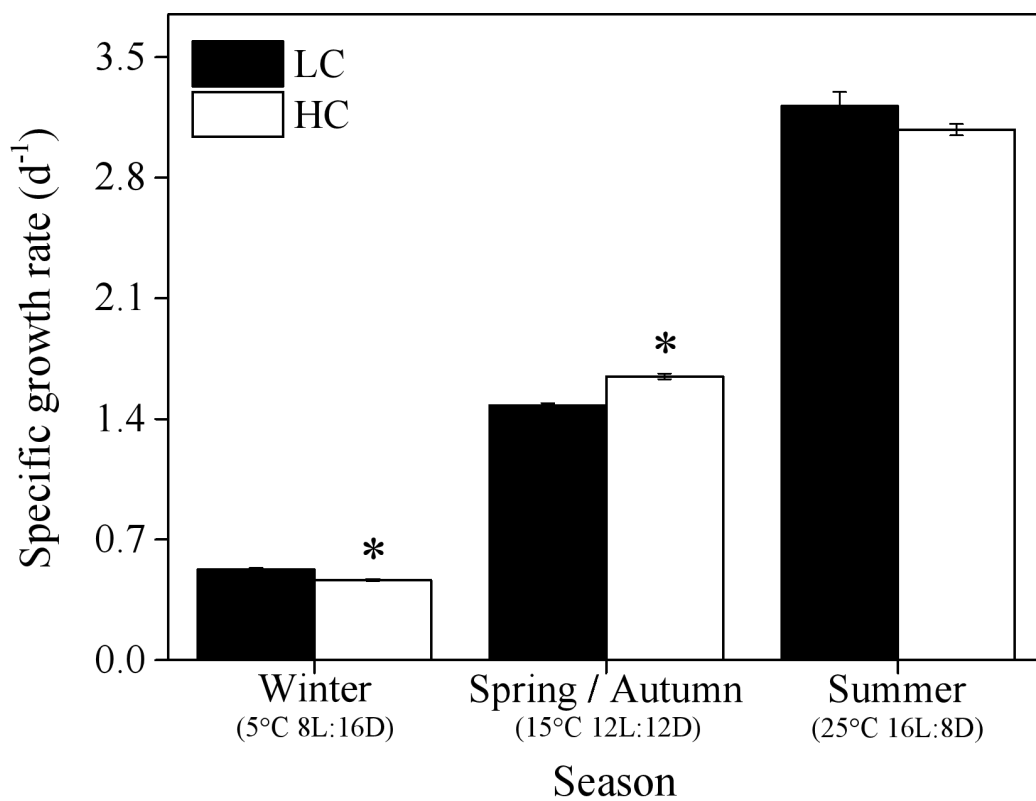
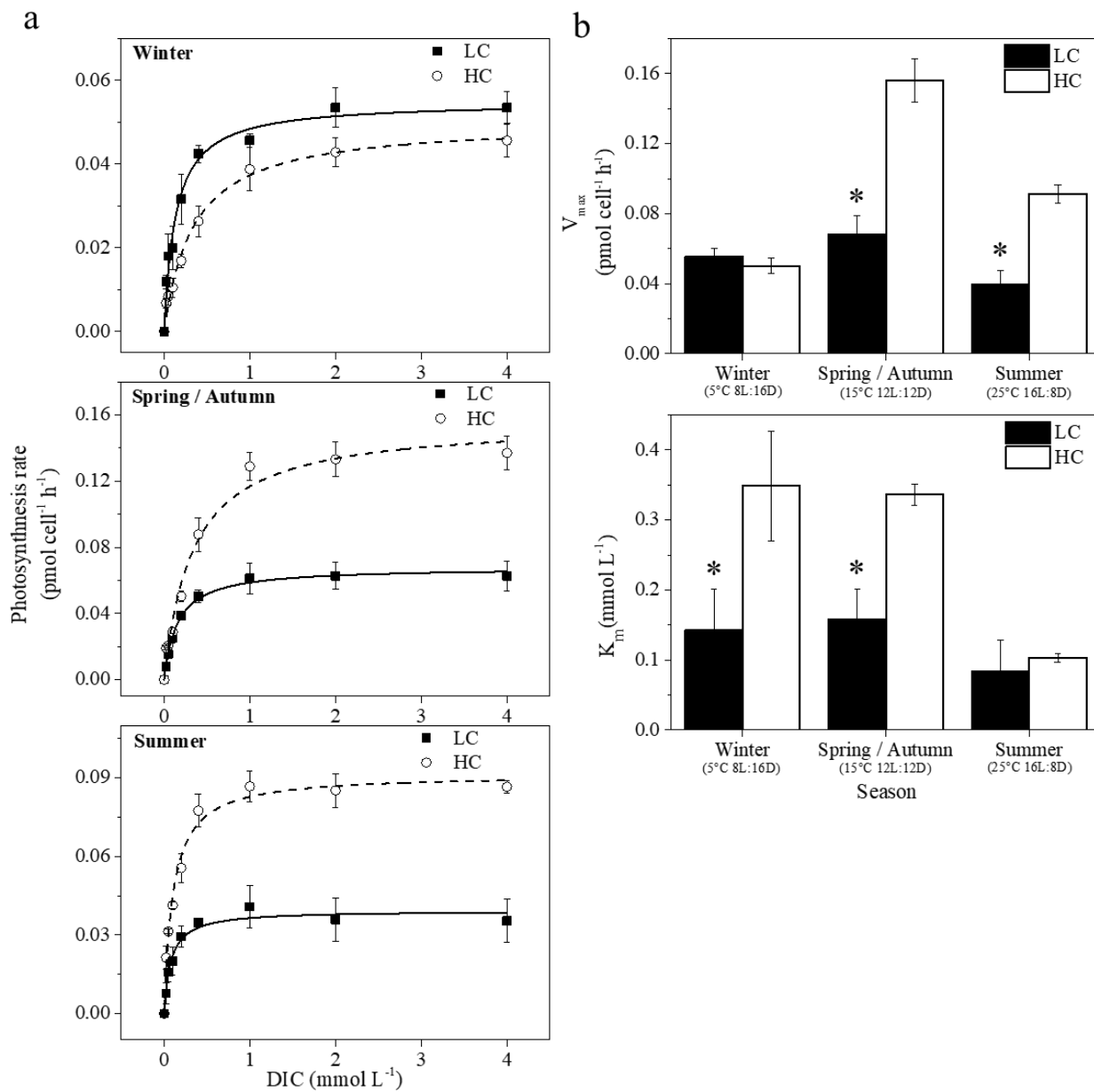


Figure 1: Specific growth rate of *S. costatum* acclimated to ambient (LC, black bars) and elevated pCO<sub>2</sub> (HC, white bars) under different combination of temperature and photoperiod conditions. The data are mean ± SD values of triplicate cultures (n = 3). Asterisks represent significant differences ( $P < 0.05$ ) between two CO<sub>2</sub> levels under same season condition (*t*-test).

430





**Figure 2:** (a) Photosynthesis-inorganic carbon ( $C_i$ ) (P-C) curves of cells acclimated to ambient and elevated  $pCO_2$  in different seasons. (b) Photosynthetic parameters of P - C curves at ambient (LC, black bars) and elevated  $pCO_2$  (HC, white bars) in different seasons.  $K_m$  is half-saturation constant and  $V_{max}$  is the inorganic carbon-saturated maximal rate of photosynthesis. The data are mean  $\pm$  SD values of triplicate cultures ( $n = 3$ ). Asterisks represent significant differences ( $P < 0.05$ ) between two  $CO_2$  levels under same season ( $t$ -test).

435

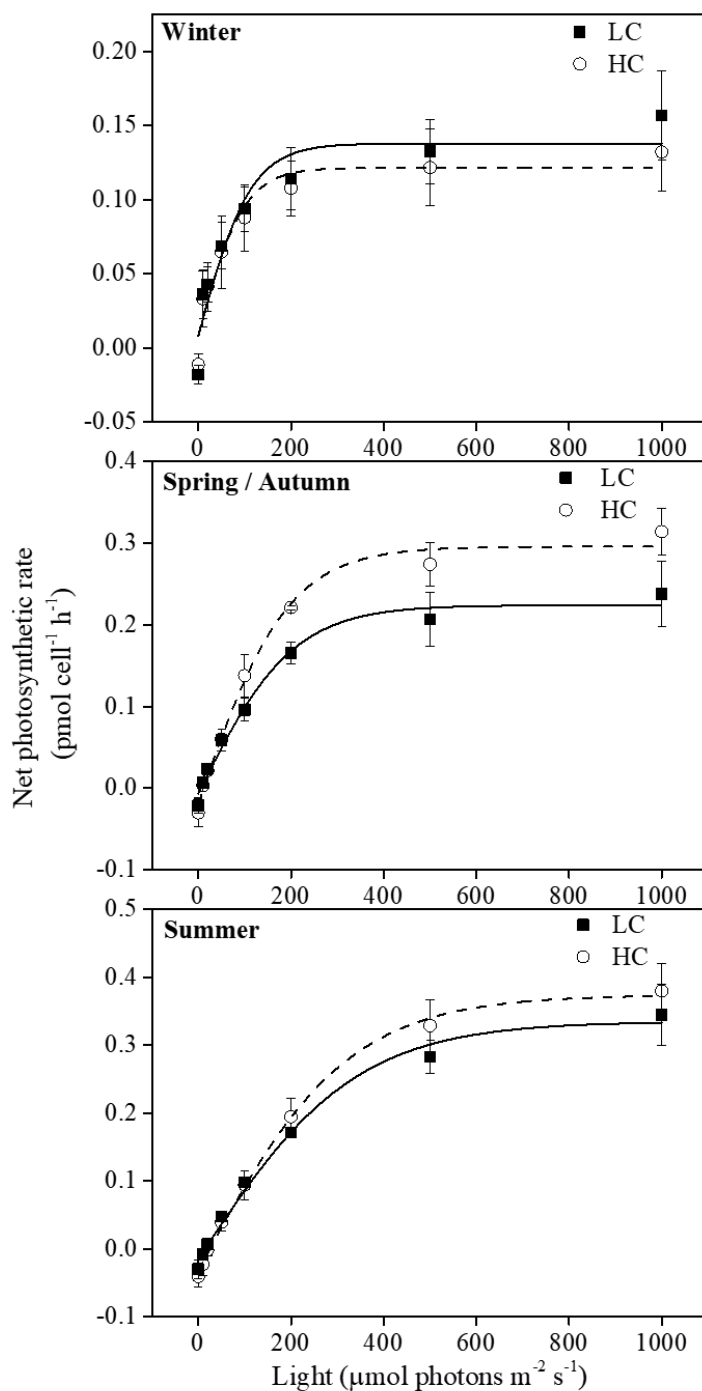
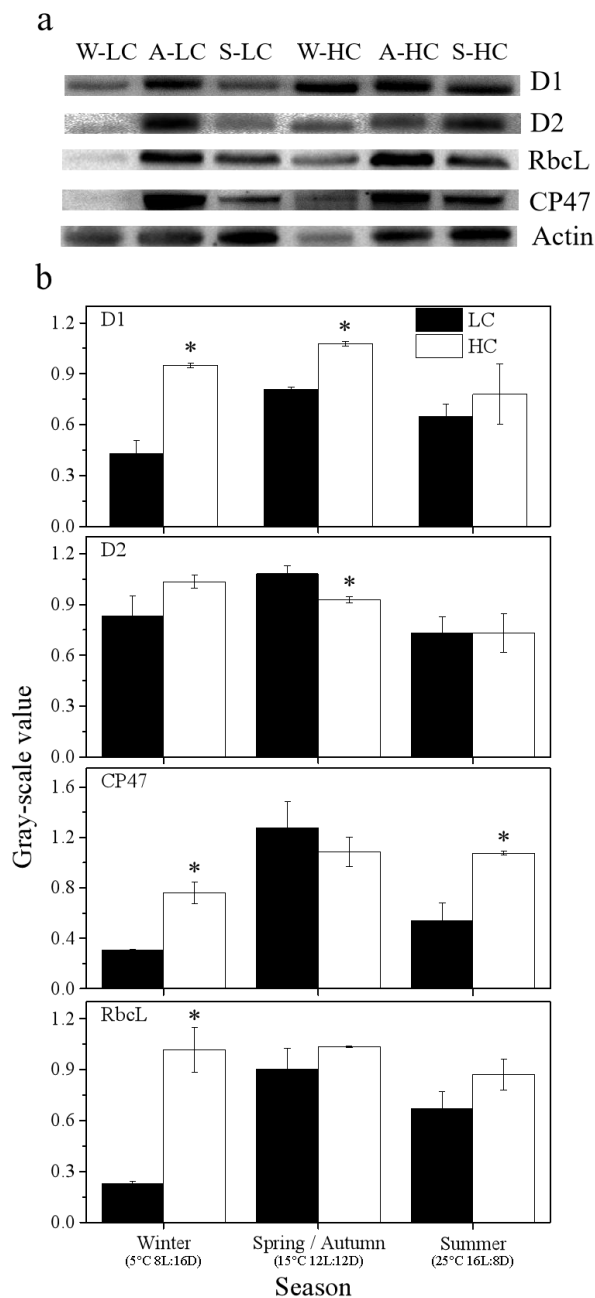


**Figure 3: Photosynthesis-light curves (P-I curves) of cells acclimated to ambient and elevated pCO<sub>2</sub> in different seasons. The data are mean ± SD values of triplicate cultures (n = 3).**



440

**Figure 4:** (a) Immunoblot using antibodies against four kinds of photosynthesis-associated proteins of thylakoids (PsbA (D1), PsbD (D2), PsbB (CP47), and RbcL) isolated from *S. costatum* acclimated to ambient and elevated pCO<sub>2</sub> in different season levels (W for winter, A for autumn, S for summer). Each line was loaded with similar amounts of proteins. (b) Quantitative analysis of proteins. The relative abundance of each band was estimated by densitometric scanning of the exposed films. Asterisks represent significant differences ( $P < 0.05$ ) between two CO<sub>2</sub> levels under same season ( $t$ -test).

445